VARIABLE CONTROL FOR IMPROVING SENSING CAPABILITY OF FLYING OBJECT

[1]WOONG LIM, [2]WOO CHUN CHOI

[1]Graduate School, Department of Mechanical Engineering, Korea University, Seoul, South Korea
[2]Department of Mechanical Engineering, Korea University, Seoul, South Korea
E-mail: [1]sinic1219@korea.ac.kr, [2]wcchoi@korea.ac.kr

Abstract- The purpose of the low-speed flying object studied here is to search a target on the ground. An IR sensor attached to the object senses a moving target on the ground. The object discharged from a platform flies with parabolic motion and precession. The IR sensor scans the ground, showing a certain trajectory on the ground. Therefore, the precession is the most important factor affecting the sensing capability. In this study, to improve the sensing capability of the flying object, governing equations are derived, and the characteristics are investigated by MATLAB numerical analysis. Also, the solution is presented for optimal sensing through variable control.

Index Terms- Dynamics, Flying Object, Precession, IR sensor, HTM.

I. INTRODUCTION

The purpose of a flying object is to search a target on the ground. Since this object searches a target in the air, it can sense a target accurately and can sense an even concealed target easily. The object is shown in Fig. 1, and sensing is done by an IR sensor attached to the target. Because the characteristics of the IR sensor is to sense a target as shown in Fig. 1, a precession is necessary.
The object is discharged from a platform, and flies with parabolic motion and precession. Due to the precession, the IR sensor draws a certain trajectory on the ground which is the footprint shown in Fig. 1. The footprint presenting sensing capability is affected by the precession.

Previously, the behavior was studied by a dynamic analysis program [1], and stabilization through variable control was done [2].
This study is done analytically. This is different from previous studies. Governing equations are derived under an ideal condition, and a solution is presented for optimal sensing.

II. GOVERNING EQUATION

A. Angular momentum equations

The following equations show the angular momentums for a rigid body having a general 3D motion.

$$\begin{aligned} H_x &= I_{xx}\omega_x - I_{xy}\omega_y - I_{zx}\omega_z \\ H_y &= -I_{xy}\omega_x + I_{yy}\omega_y - I_{yz}\omega_z \\ H_z &= -I_{zx}\omega_x - I_{yz}\omega_y + I_{zz}\omega_z \end{aligned} \quad (1)$$

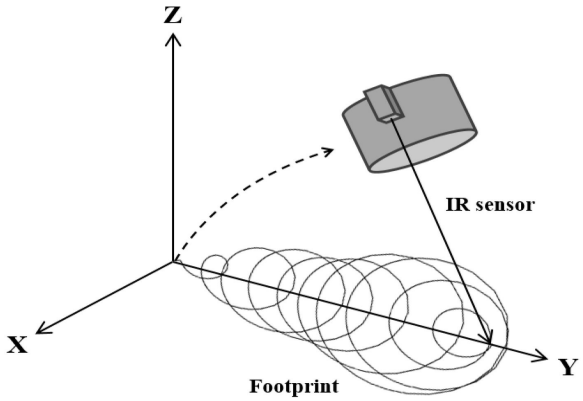


Fig. 1 Flight object and footprint

Differentiating equation (1) gives

$$\begin{aligned} \dot{H}_x &= I_{xx}\dot{\omega}_x - I_{xy}\dot{\omega}_y - I_{zx}\dot{\omega}_z \\ \dot{H}_y &= -I_{xy}\dot{\omega}_x + I_{yy}\dot{\omega}_y - I_{yz}\dot{\omega}_z \\ \dot{H}_z &= -I_{zx}\dot{\omega}_x - I_{yz}\dot{\omega}_y + I_{zz}\dot{\omega}_z \end{aligned} \quad (2)$$

In equations (1) and (2), I_{xx}, I_{yy}, I_{zz} are moment of inertia, and I_{xy}, I_{yz}, I_{zx} are product of inertia.

B. Moment equations

When The relation between moments and angular momentums in x, y, and z directions is

$$\begin{aligned} \Sigma M_x &= \dot{H}_x - H_y\omega_z + H_z\omega_y \\ \Sigma M_y &= \dot{H}_y - H_z\omega_x + H_x\omega_z \\ \Sigma M_z &= \dot{H}_z - H_x\omega_y + H_y\omega_x \end{aligned} \quad (3)$$

C. Eulerian angle equations

Fig. 2 shows coordinate systems used for the flying object. XYZ and xyz coordinate systems in Fig. 2 (a) represent the global and local coordinate systems, respectively. The global coordinate is independent from the object, and the local coordinate is fixed onto the object.

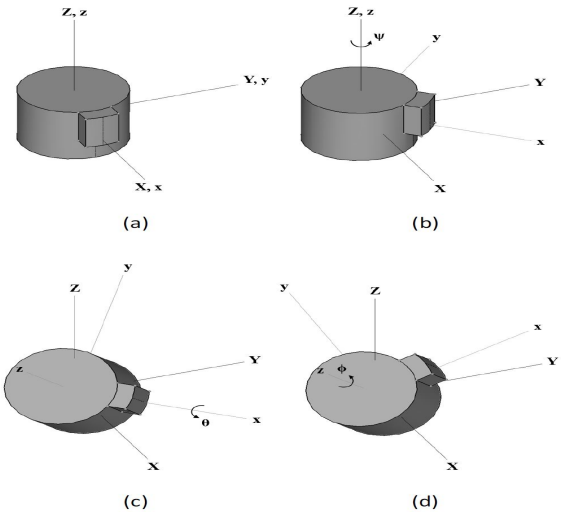


Fig. 2 Global and local coordinates

Without translational motion, any rotational angles of the local coordinate with respect to the global coordinate can be represented by Eulerian angles ψ, θ, ϕ. ψ is a precession angle, rotation of the local coordinate with respect to the global Z axis. θ is a nutation angle, rotation of the local coordinate with respect to the local x axis as shown in Fig. 2 (c). ϕ is spin angle, rotation of the local coordinate with respect to the local z axis. Angular speed and angular acceleration in x, y and z axes are presented by Eulerian angles.

$$\begin{aligned} \omega_x &= \dot{\psi}\sin\theta\sin\phi + \dot{\theta}\cos\phi \\ \omega_y &= \dot{\psi}\sin\theta\cos\phi - \dot{\theta}\sin\phi \\ \omega_z &= \dot{\psi}\cos\theta + \dot{\phi} \end{aligned} \quad (4)$$

$$\begin{aligned} \dot{\omega}_x &= \ddot{\psi}\sin\theta\sin\phi + \dot{\psi}\dot{\theta}\cos\theta\sin\phi \\ &\quad + \dot{\psi}\dot{\phi}\sin\theta\cos\phi + \ddot{\theta}\cos\phi - \dot{\theta}\dot{\phi}\sin\phi \\ \dot{\omega}_y &= \ddot{\psi}\sin\theta\cos\phi + \dot{\psi}\dot{\theta}\cos\theta\cos\phi \\ &\quad - \dot{\psi}\dot{\phi}\sin\theta\sin\phi - \ddot{\theta}\sin\phi - \dot{\theta}\dot{\phi}\cos\phi \\ \dot{\omega}_z &= \ddot{\psi}\cos\theta - \dot{\psi}\dot{\theta}\sin\theta + \ddot{\phi} \end{aligned} \quad (5)$$

D. Governing equations

Equations (1), (2), (4) and (5) are substituted into equation (3). Then, moment equations are obtained for ideal condition.

Table 1 Initial conditions

θ (rad)	$\dot{\theta}$ (rad/s)	ψ (rad)	$\dot{\psi}$ (rad/s)	ϕ (rad)	$\dot{\phi}$ (rad/s)
0.6998	0	0.0813	31.4159	0.8104	24.0332

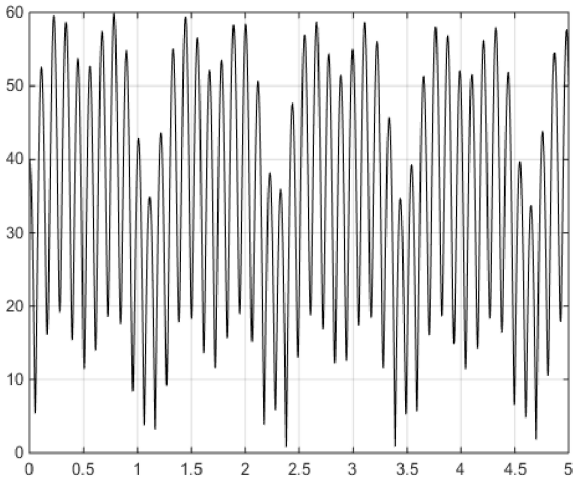


Fig. 3 Numerical analysis result of θ

III. NUMERICAL ANALYSIS

Since the object flies without any constraint, the three moments are '0'. In order to solve the ordinary differential equation, $\ddot{\psi}, \ddot{\theta}, \ddot{\phi}$ are represented by ψ, θ, ϕ and $\dot{\psi}, \dot{\theta}, \dot{\phi}$ from the three equations. The equation is very complicated, and numerical analysis is done using MATLAB. The initial condition is shown in Table 1. Fig. 3 shows the result of θ affecting sensing most.

IV. FOOTPRINT

The flying object is discharged from a platform, and flies with parabolic motion and precession. If the precession does not affect the parabolic motion, the parabolic motion and precession are independent from each other. Thus, parabolic motion can be added to the rotational motion. The behavior of the object can be solved. With the gravitation, the parabolic motion is represented by the following equations.

$$Y = V_0 t\cos(\alpha) \quad (6)$$

$$Z = V_0 t\sin(\alpha) - \frac{1}{2}gt^2 \quad (7)$$

Where α is discharge angle, angle between discharge direction and the horizontal direction. V_0 is the initial discharge speed. The initial values of α and V_0 are 40 $^{\circ}$and 40m/s, respectively.

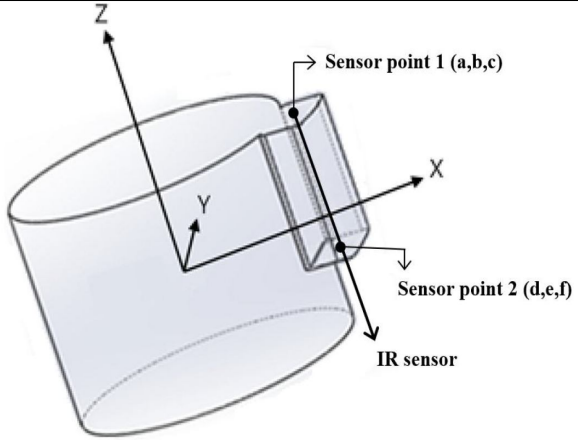


Fig. 4 Flight object and sensor point

In order to find footprint, two sensor points are used as shown in Fig. 4. The line connecting the two sensor points reaches the ground when Z is '0'. The coordinates of X and Y are

$$X = \frac{c(a-d)}{c-f} + a \tag{8}$$

$$Y = \frac{c(b-e)}{c-f} + b \tag{9}$$

Since the object has parabolic and precession motions, the coordinates (a,b,c) and (d,e,f) of the sensor points are constant in the local coordinate system, but they vary in the global coordinate system. Therefore, the positions of the sensor points have to be obtained in the global coordinate system.

In Fig. 2, five coordinate systems are used. There are three coordinate systems after rotations, global and one coordinate system with parabolic motion. Thus, four homogeneous transformation matrices from the local to the global coordinate system are needed, and they are multiplied orderly. Fig. 5 shows the result with the initial condition shown in Table 1.

V. TILTING ANGLE OPTIMIZATION

A. Variable selection

The object is discharged with initial three angles. The first angle is discharge angle α , angle between the local y axis and the global XY plane as shown in Fig. 2. The second angle is tilting angle β , angle between the local z axis and global YZ plane. The third angle is rotation angle γ , angle with respect to the local z axis.

As shown in Fig. 5, the foot print varies, depending on the three angles. With different values of the angles, numerical analysis was done, and the tilting angle was found to be the most important factor affecting the footprint shape. The initial values of the discharge angle and the rotation angle were set at 40 °, 50 °, and the tilting angle was varied.

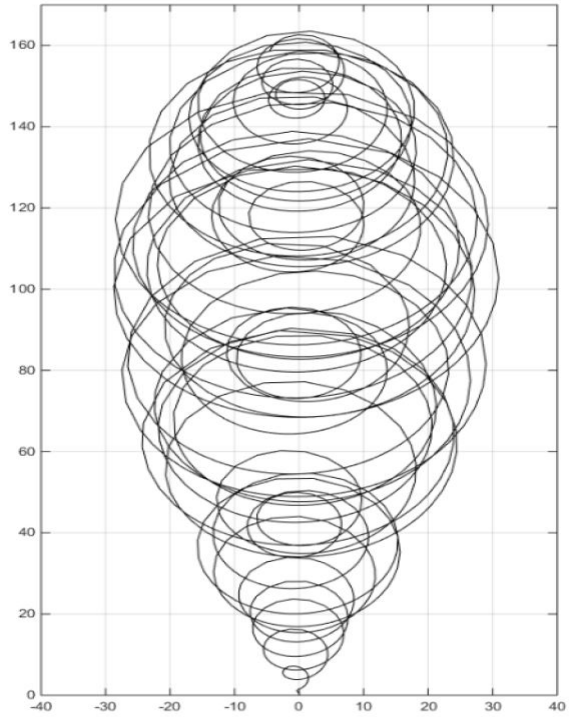


Fig. 5 Footprint

Table 2 Three variables and Eulerian angles

α (deg)	β (deg)	γ (deg)	θ (deg)	ψ (deg)	ϕ (deg)
40	-30	50	48.439	123.826	83.122
40	-27	50	46.957	124.941	81.561
40	-24	50	45.588	125.960	79.951
40	-21	50	44.343	126.877	78.295
40	-18	50	43.235	127.686	76.595
40	-15	50	42.274	128.381	74.853
40	-12	50	41.470	128.957	73.072
40	-9	50	40.833	129.411	71.254
40	-6	50	40.373	129.737	69.400
40	-3	50	40.093	129.934	67.514
40	0	50	40.000	130.000	65.596
40	3	50	40.093	129.934	63.648
40	6	50	40.373	129.737	61.672
40	9	50	40.833	129.411	59.670
40	12	50	41.470	128.957	57.644
40	15	50	42.274	128.381	55.594
40	18	50	43.235	127.686	53.522
40	21	50	44.343	126.877	51.430
40	24	50	45.588	125.960	49.318
40	27	50	46.957	124.941	47.189
40	30	50	48.439	123.826	45.042

B. Eulerian angles

In order to do numerical analysis, the three angles have to be presented by Eulerian angles. The variable was the tilting angle, and footprint was obtained. Table 2 shows the Eulerian angles for various tilting

angles.

Table 3 Final initial conditions

θ (rad)	$\dot{\theta}$ (rad/s)	ψ (rad)	$\dot{\psi}$ (rad/s)	ϕ (rad)	$\dot{\phi}$ (rad/s)
0.8454	0	-0.7318	31.4159	1.4101	20.8419
0.8196	0	-0.6703	31.4159	1.3686	21.4428
0.7957	0	-0.6058	31.4159	1.3240	21.9853
0.7739	0	-0.5383	31.4159	1.2763	22.4677
0.7546	0	-0.4680	31.4159	1.2255	22.8881
0.7378	0	-0.3950	31.4159	1.1719	23.2458
0.7238	0	-0.3194	31.4159	1.1156	23.5400
0.7127	0	-0.2415	31.4159	1.0570	23.7699
0.7046	0	-0.1621	31.4159	0.9966	23.9340
0.6998	0	-0.0813	31.4159	0.9350	24.0332
0.6981	0	0.0000	31.4159	0.8727	24.0660
0.6998	0	0.0813	31.4159	0.8104	24.0332
0.7046	0	0.1621	31.4159	0.7487	23.9340
0.7127	0	0.2415	31.4159	0.6883	23.7699
0.7238	0	0.3194	31.4159	0.6298	23.5400
0.7378	0	0.3950	31.4159	0.5735	23.2458
0.7546	0	0.4680	31.4159	0.5198	22.8881
0.7739	0	0.5383	31.4159	0.4690	22.4677
0.7957	0	0.6058	31.4159	0.4213	21.9853
0.8196	0	0.6703	31.4159	0.3768	21.4428
0.8454	0	0.7318	31.4159	0.3353	20.8419

C. Initial conditions

Finally, initial values of $\dot{\theta}, \dot{\psi}, \dot{\phi}$ were set. The initial value of $\dot{\theta}$ was set at '0', because there is no acceleration for nutation angle. $\dot{\psi}$ was set at 5 rps. $\dot{\phi}$ is $\dot{\psi}\cos(\theta)$. The initial conditions are shown in Table 3.

D. Tilting angle for stable sensing

The goal is to find the tilting angle resulting in better sensing capability. Good sensing capability requires the followings:

1. The footprint should be symmetric.
2. The footprint should have as small difference between maximum and minimum widths in the footprint like in Fig. 5 as possible.

In Fig. 5, a right amplitude is defined as the rightmost value of each path, and a left amplitude is defined as the leftmost value of each path. The second criterion is a biased amplitude, which can be represented as the sum of average right and left amplitudes. It means the degree of bias of the sensing trajectory.

To find the behavior for tilting angle, numerical analysis was done with initial conditions shown in Table 3.

All the results showed similar behaviors like Fig. 3, and variation frequencies were almost the same. However, the difference between maximum and minimum widths varied significantly. Thus, θ resulting in the smallest difference was to be found, with symmetric shape.

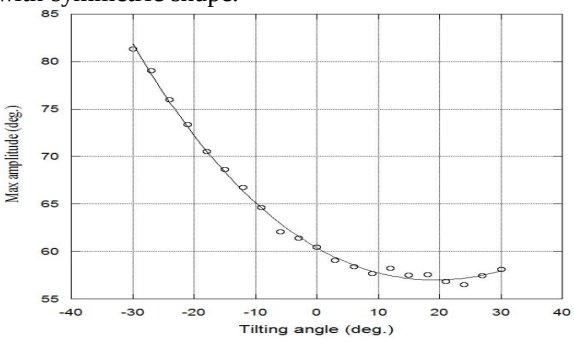


Fig. 6 Tilting angle and max amplitude of θ

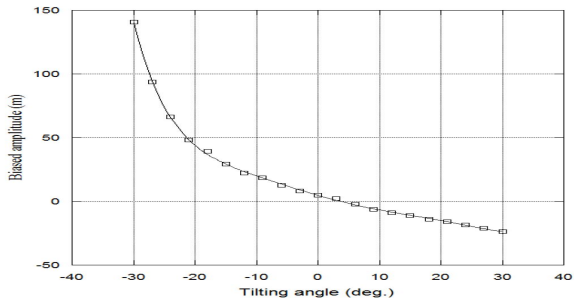


Fig. 7 Tilting angle and footprint biased distance

Fig. 6 shows the maximum amplitude of θ. This is the maximum width of θ shown in Fig. 3. In Fig. 6, the tilting angle resulting in the minimum amplitude is 15~20 °. Fig. 7 shows the second criterion.

For good sensing capability, the footprint should be symmetric, and the tilting angle having the smallest biased amplitude should be found. The value was found to be 3.55 °by curve fitting. For the tilting angle, the amplitude was 59.22 °. this value is greater than the minimum amplitude 56.48 °by 2.74 °.

VI. EFFECT OF RPS

The acceptable range of $\dot{\psi}$ is 5~10 rps. If it is smaller than 5 rps, the space of the footprint becomes large and the sensing capability declines. If it is greater than 10, the sensor cannot sense a target because of excessive speed. In the acceptable range, the behavior of θ was found for $\dot{\psi}$ variation. Initial conditions of α, β, γ were 40 °, 3.55 °, 50 °. The results are shown in Figs. 8 and 9. From Figs. 6-9, the contribution of $\dot{\psi}$ to θ is low.

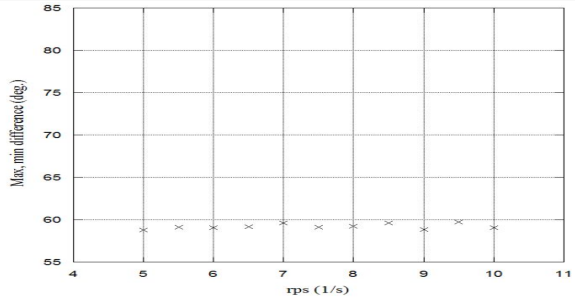


Fig. 8 Precession speed and max amplitude of θ

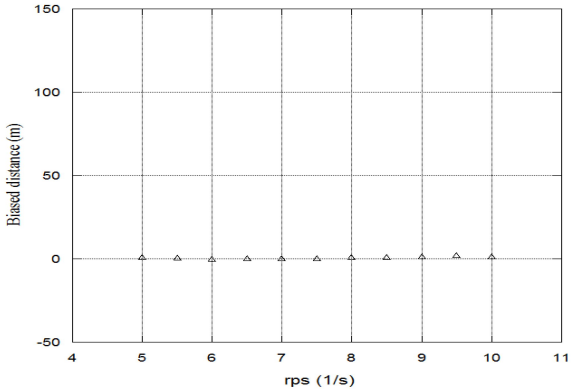


Fig. 9 Precession speed and footprint biased distance

CONCLUSIONS

Under ideal condition, governing equations were derived from angular momentum equations, angular speed equations and angular acceleration equations. The ordinary differential equations were solved using MATLAB, and the dynamic behavior of the object was investigated. Aerodynamic effects were not considered. These effects will be included in the future study. In this study, the following conclusions were drawn.

- Governing equations were obtained for dynamic behavior of an object using Eulerian angles.
- The orientation of the object was solved using MATLAB, and the footprint of the sensor was obtained.
- The variable affecting the footprint most was found.
- The tilting angle resulting symmetric footprint was 3.55 °, and the maximum amplitude of θ was 59.22 °.

ACKNOWLEDGMENT

This study is supported by the Korea Evaluation Institute of Industrial Technology (10043477) and the BK21 plus program(21A20131712520) through the National Research Foundation(NRF) funded by the Ministry of Education of Korea.

REFERENCES

[1] S. H. Jung, S. S. Park, J. H. Bong, H. K. Lee, I. K. Kim, “Control and Analysis of the Principal Motion’s Stability Variables in the Low Speed System,” in KSPE, vol. 2014, no. 10, 2014.

[2] S. H. Jung, S. S. Park, J. H. Bong, I. K. Kim, H. I. Song, H. K. Lee, “Dynamic Control and Analysis for Precession of Low Speed Flight Object,” in KSPE, vol. 2013, no. 10, 2013.

★★★